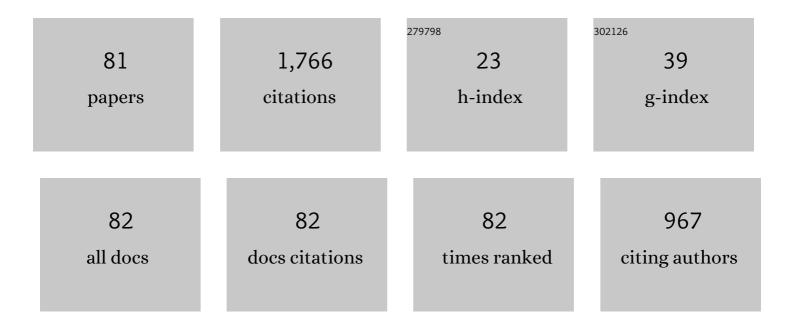
List of Publications by Year in descending order

Source: https://exaly.com/author-pdf/2765756/publications.pdf Version: 2024-02-01



#	Article	IF	CITATIONS
1	Constitutive model for high temperature deformation of titanium alloys using internal state variables. Mechanics of Materials, 2010, 42, 157-165.	3.2	122
2	The growth behavior of austenite grain in the heating process of 300M steel. Materials Science & Engineering A: Structural Materials: Properties, Microstructure and Processing, 2011, 528, 4967-4972.	5.6	109
3	High temperature deformation behavior of a near alpha Ti600 titanium alloy. Materials Science & Engineering A: Structural Materials: Properties, Microstructure and Processing, 2008, 492, 24-28.	5.6	88
4	Surface nanocrystallization and gradient structure developed in the bulk TC4 alloy processed by shot peening. Journal of Alloys and Compounds, 2016, 685, 186-193.	5.5	87
5	Effect of the strain on the deformation behavior of isothermally compressed Ti–6Al–4V alloy. Materials Science & Engineering A: Structural Materials: Properties, Microstructure and Processing, 2009, 505, 88-95.	5.6	83
6	High temperature deformation behavior of near alpha Ti–5.6Al–4.8Sn–2.0Zr alloy. Journal of Materials Processing Technology, 2007, 183, 71-76.	6.3	81
7	Nanostructure and surface roughness in the processed surface layer of Ti-6Al-4V via shot peening. Materials Characterization, 2017, 123, 83-90.	4.4	76
8	The modelling of dynamic recrystallization in the isothermal compression of 300M steel. Materials Science & Engineering A: Structural Materials: Properties, Microstructure and Processing, 2013, 574, 1-8.	5.6	69
9	The gradient crystalline structure and microhardness in the treated layer of TC17 via high energy shot peening. Applied Surface Science, 2015, 357, 197-203.	6.1	55
10	Effect of the strain on processing maps of titanium alloys in isothermal compression. Materials Science & Engineering A: Structural Materials: Properties, Microstructure and Processing, 2009, 504, 90-98.	5.6	52
11	Nanocrystallization mechanism of beta phase in Ti-6Al-4V subjected to severe plastic deformation. Materials Science & Engineering A: Structural Materials: Properties, Microstructure and Processing, 2016, 669, 7-13.	5.6	45
12	Effect of 0.770wt%H addition on the microstructure of Ti–6Al–4V alloy and mechanism of l´ hydride formation. Journal of Alloys and Compounds, 2009, 481, 480-485.	5.5	42
13	Modeling of void closure in diffusion bonding process based on dynamic conditions. Science China Technological Sciences, 2012, 55, 2420-2431.	4.0	38
14	Structure response characteristics and surface nanocrystallization mechanism of alpha phase in Ti-6Al-4V subjected to high energy shot peening. Journal of Alloys and Compounds, 2019, 773, 860-871.	5.5	38
15	Effect of hydrogenation content on high temperature deformation behavior of Ti–6Al–4V alloy in isothermal compression. International Journal of Hydrogen Energy, 2008, 33, 2714-2720.	7.1	35
16	Constitutive model and optimal processing parameters of TC17 alloy with a transformed microstructure via kinetic analysis and processing maps. Materials Science & Engineering A: Structural Materials: Properties, Microstructure and Processing, 2017, 698, 302-312.	5.6	34
17	Microstructural evolution and modelling of the hot compression of a TC6 titanium alloy. Materials Characterization, 2002, 49, 203-209.	4.4	33
18	Detailed Evolution Mechanism of Interfacial Void Morphology in Diffusion Bonding. Journal of Materials Science and Technology, 2016, 32, 259-264.	10.7	32

#	Article	IF	CITATIONS
19	Grain refinement in near alpha Ti60 titanium alloy by the thermohydrogenation treatment. International Journal of Hydrogen Energy, 2007, 32, 626-629.	7.1	30
20	Bonding interface characteristic and shear strength of diffusion bonded Ti-17 titanium alloy. Transactions of Nonferrous Metals Society of China, 2015, 25, 80-87.	4.2	28
21	Effect of Processing Parameters on Microstructure and Mechanical Properties in High Temperature Deformation of Ti-6Al-4V Alloy. Rare Metal Materials and Engineering, 2009, 38, 19-24.	0.8	27
22	Lattice variations of Ti-6Al-4V alloy with hydrogen content. Materials Characterization, 2011, 62, 724-729.	4.4	27
23	Evolution mechanisms of the primary α and β phases during α/β deformation of an α/β titanium alloy TC8. Materials Characterization, 2016, 120, 115-123.	4.4	27
24	Microscopic observation of cold-deformed Al–4Cu–Mg alloy samples after semi-solid heat treatments. Materials Characterization, 2005, 54, 451-457.	4.4	22
25	Influence of pressure on interfacial microstructure evolution and atomic diffusion in the hot-press bonding of Ti-33Al-3V to TC17. Journal of Alloys and Compounds, 2017, 720, 131-138.	5.5	22
26	Modeling of constitutive relationships and microstructural variables of Ti–6.62Al–5.14Sn–1.82Zr alloy during high temperature deformation. Materials Characterization, 2008, 59, 1386-1394.	4.4	21
27	Effect of 0.16wt% hydrogen addition on high temperature deformation behavior of the Ti600 titanium alloy. Materials Science & Engineering A: Structural Materials: Properties, Microstructure and Processing, 2009, 513-514, 228-232.	5.6	21
28	Characteristics and formation mechanisms of defects in surface layer of TC17 subjected to high energy shot peening. Applied Surface Science, 2020, 509, 144711.	6.1	21
29	Deformation behavior and microstructural evolution during the semi-solid compression of Al–4Cu–Mg alloy. Materials Characterization, 2005, 54, 423-430.	4.4	19
30	Microstructure and mechanical properties of heat-treated Ti–5Al–2Sn–2Zr–4Mo–4Cr. Transactions of Nonferrous Metals Society of China, 2015, 25, 2893-2900.	4.2	19
31	Deformation mechanisms of nanocrystalline alpha titanium in Ti-6Al-4V. Materials Letters, 2016, 185, 488-490.	2.6	16
32	Effect of hydrogen addition on the microstructure of TC21 alloy. Materials Science & Engineering A: Structural Materials: Properties, Microstructure and Processing, 2010, 527, 7080-7085.	5.6	15
33	Prediction of flow stress in isothermal compression of Ti–6Al–4V alloy using fuzzy neural network. Materials & Design, 2010, 31, 3078-3083.	5.1	15
34	Finite Element Simulation of Deformation Behavior in Friction Welding of Al-Cu-Mg Alloy. Journal of Materials Engineering and Performance, 2006, 15, 627-631.	2.5	13
35	Deformation Behavior of TC6 Alloy in Isothermal Forging. Journal of Materials Engineering and Performance, 2005, 14, 671-676.	2.5	12
36	Evolution characterization of α lamellae during isothermal compression of TC17 alloy with colony-α microstructure. Materials Science & Engineering A: Structural Materials: Properties, Microstructure and Processing, 2018, 712, 637-644.	5.6	12

#	Article	IF	CITATIONS
37	Twinning and twin intersections in γ grains of Ti-42.9Al-4.6Nb-2Cr. Journal of Materials Science and Technology, 2021, 88, 90-98.	10.7	12
38	Diffusion bonding of dissimilar titanium alloys via surface nanocrystallization treatment. Journal of Materials Research and Technology, 2022, 17, 1274-1288.	5.8	12
39	Application of Thermohydrogen Processing for Formation of Ultrafine Equiaxed Grains in Near α Ti600 Alloy. Metallurgical and Materials Transactions A: Physical Metallurgy and Materials Science, 2009, 40, 3009-3015.	2.2	11
40	Stress-induced twinning of nanocrystalline hexagonal close-packed titanium in Ti-6Al-4V. Materials Letters, 2016, 180, 47-50.	2.6	11
41	Plastic flow behavior of superalloy GH696 during hot deformation. Transactions of Nonferrous Metals Society of China, 2016, 26, 712-721.	4.2	10
42	Deformation behavior and processing maps during isothermal compression of TC21 alloy. Rare Metals, 2017, 36, 86-94.	7.1	10
43	Further refinement mechanisms of nanograins in nanocrystalline surface layer of TC17 subjected to severe plastic deformation. Applied Surface Science, 2021, 538, 147941.	6.1	10
44	Optimization of TC11 alloy forging parameters using processing maps. Rare Metals, 2011, 30, 222-226.	7.1	9
45	Grain size model for continuous dynamic recrystallization of titanium alloy in hot deformation. Science China Technological Sciences, 2018, 61, 1688-1695.	4.0	9
46	Fabrication and Microstructure Evolution of Semi-Solid LY11 Alloy by SIMA. Journal of Materials Engineering and Performance, 2003, 12, 249-253.	2.5	8
47	Acquiring a Novel Constitutive Equation of a TC6 Alloy at High-Temperature Deformation. Journal of Materials Engineering and Performance, 2005, 14, 263-266.	2.5	8
48	A set of microstructure-based constitutive equations in hot forming of a titanium alloy. International Journal of Minerals, Metallurgy, and Materials, 2006, 13, 435-441.	0.2	8
49	Deformation Behavior in the Isothermal Compression of Hydrogenated Ti–5.6Al–4.8Sn–2.0Zr–1.0Mo Alloy. Journal of Materials Engineering and Performance, 2007, 16, 93-96.	2.5	8
50	Thermomechanical coupling simulation and experimental study in the isothermal ECAP processing of Ti-6Al-4V alloy. Rare Metals, 2010, 29, 613-620.	7.1	8
51	Modeling of grain size in isothermal compression of Ti-6Al-4V alloy using fuzzy neural network. Rare Metals, 2011, 30, 555-564.	7.1	8
52	Variation effect of strain rate on microstructure in isothermal compression of Ti-6Al-4V alloy. Rare Metals, 2012, 31, 7-11.	7.1	8
53	Microstructure evolution and its effect on flow stress of TC17 alloy during deformation in $\hat{1}_{\pm}+\hat{1}^2$ two-phase region. Transactions of Nonferrous Metals Society of China, 2019, 29, 1430-1438.	4.2	8
54	Microstructure and Element Distribution during Partial Remelting of an Al-4Cu-Mg alloy. Journal of Materials Engineering and Performance, 2008, 17, 25-29.	2.5	7

#	Article	IF	CITATIONS
55	High-Temperature Deformation Behavior of Ti-6Al-4V Alloy without and with Hydrogenation Content of 0.27 wt.%. Journal of Materials Engineering and Performance, 2010, 19, 59-63.	2.5	7
56	Kinetic analysis and strain-compensated constitutive models of Ti-42.9Al-4.6Nb–2Cr during isothermal compression. Progress in Natural Science: Materials International, 2020, 30, 260-269.	4.4	7
57	Microstructure evolution in the high temperature compression of Ti-5.6Al-4.8Sn-2.0Zr alloy. Rare Metals, 2010, 29, 533-537.	7.1	6
58	3D finite element simulation of microstructure evolution in blade forging of Ti-6Al-4V alloy based on the internal state variable models. International Journal of Minerals, Metallurgy and Materials, 2012, 19, 122-130.	4.9	6
59	High Temperature Behavior of Isothermally Compressed M50 Steel. Journal of Iron and Steel Research International, 2015, 22, 969-976.	2.8	6
60	Three-dimensional Numerical Simulation and Experimental Analysis of Austenite Grain Growth Behavior in Hot Forging Processes of 300M Steel Large Components. Journal of Iron and Steel Research International, 2016, 23, 1012-1019.	2.8	6
61	Metadynamic recrystallization of 300M steel after isothermal compression. Materials at High Temperatures, 2017, 34, 279-288.	1.0	6
62	Quantitative characterization of β-solidifying γ-TiAl alloy with duplex structure. Transactions of Nonferrous Metals Society of China, 2021, 31, 1993-2004.	4.2	6
63	Kinetic variables based constitutive model for high temperature deformation of Ti-46.5Al–2Nb–2Cr. Journal of Materials Research and Technology, 2021, 15, 3525-3537.	5.8	6
64	Deformation Behavior and Constitutive Equation Coupled the Grain Size of Semi-Solid Aluminum Alloy. Journal of Materials Engineering and Performance, 2010, 19, 1337-1343.	2.5	5
65	Formation of adiabatic shear band and deformation mechanisms during warm compression of Ti–6Al–4V alloy. Rare Metals, 2016, 35, 598-605.	7.1	5
66	Significance and interaction of bonding parameters with bonding ratio in press bonding of TC4 alloy. Rare Metals, 2016, 35, 235-241.	7.1	5
67	Prediction model for flow stress during isothermal compression in αÂ+Âβ phase field of TC4 alloy. Rare Metals, 2018, 37, 369-375.	7.1	5
68	Microscopic characterization of semi-solid aluminium alloys. International Journal of Minerals, Metallurgy and Materials, 2010, 17, 290-296.	4.9	4
69	Quantitative analysis on microstructure evolution of Ti-6Al-2Zr-2Sn-2Mo-1.5Cr-2Nb alloy during isothermal compression. Rare Metals, 2015, 34, 625-631.	7.1	4
70	Dynamic Recrystallization-Related Interface Phase Boundary Migration of TC17/TC4 Bond with Initial Equiaxed Microstructure. Jom, 2019, 71, 2253-2261.	1.9	4
71	Quantitative analysis of globularization and modeling of TC17 alloy with basketweave microstructure. Transactions of Nonferrous Metals Society of China, 2022, 32, 850-867.	4.2	4
72	FE-based coupling simulation of Ti60 alloy in isothermal upsetting process. Transactions of Nonferrous Metals Society of China, 2010, 20, 849-856.	4.2	3

#	Article	IF	CITATIONS
73	Prediction model for surface layer microhardness of processed TC17 via high energy shot peening. Transactions of Nonferrous Metals Society of China, 2017, 27, 1956-1963.	4.2	3
74	Fragmentation of α Grains Accelerated by the Growth of β Phase in Ti–5Al–2Sn–2Zr–4Mo–4Cr during Hot Deformation. Advanced Engineering Materials, 2018, 20, 1700200.	3.5	3
75	Sensitivity analysis on globularized fraction of α lamellae in titanium alloys. Transactions of Nonferrous Metals Society of China, 2019, 29, 305-312.	4.2	3
76	Characterization of crystal structure in the bonding interface between TC17 and TC4 alloys. Materials Characterization, 2019, 153, 169-174.	4.4	3
77	Effect of processing parameters on flow behaviors and microstructure during high temperature deformation of GH4586 superalloy. Journal of Central South University, 2021, 28, 338-350.	3.0	3
78	The role of β phase in the morphology evolution of α lamellae in a dual-phase titanium alloy during high temperature compression. Journal of Alloys and Compounds, 2022, 910, 164901.	5.5	3
79	Internal state variable models for microstructure in high temperature deformation of titanium alloys. Science in China Series D: Earth Sciences, 2008, 51, 1921-1929.	0.9	2
80	Effect of hydrogenation on the microstructure of Ti-5.6Al-4.8Sn-2.0Zr alloy. Rare Metals, 2009, 28, 343-345.	7.1	0
81	Interfacial Microstructure Characteristics and Mechanical Properties of a Press Bonded Ti–5Al–2Sn–2Zr–4Mo–4Cr Alloy. Crystals, 2021, 11, 1395.	2.2	0